

Increased Deltoid and Acromial Stress with Glenoid Lateralization and Onlay Humeral Stem Constructs in Reverse Shoulder Arthroplasty

Journal of Shoulder and Elbow Arthroplasty
Volume 8: 1–11
© The Author(s) 2024
Article reuse guidelines:
sagepub.com/journals-permissions
DOI: 10.1177/24715492241291311
journals.sagepub.com/home/sea



Brendan M Patterson, MD, MPH¹, Joshua E Johnson, PhD¹,
Maria Bozoghlian, MD¹  and Donald D Anderson, PhD¹ 

Abstract

Background: Reverse shoulder arthroplasty (RSA) designs include multiple options for glenoid component lateralization, and humeral component lateralization and distalization (inlay/onlay constructs). The influence of combined glenoid lateralization, and humeral distalization on acromial and deltoid stresses is not well understood. The purpose of this study was to evaluate changes in deltoid and acromial stresses with variations in glenoid lateralization, and with inlay versus onlay humeral components in RSA.

Methods: Finite element analysis was performed using a RSA system with both inlay and onlay configurations. Variations in total glenoid lateralization from 3 to 9 mm were evaluated. Deltoid and acromial stresses were determined following virtual implantation and with 50° of external rotation.

Results: Increased glenoid lateralization resulted in greater stress of the deltoid and acromion. There was a modest increase in deltoid stress with glenoid lateralization alone (7% and 7.5% with progressive lateralization from 3 to 6 mm and 6 to 9 mm, respectively), but deltoid stress increased substantially with use of an onlay construct (60% at 9 mm of glenoid lateralization). Acromial stress correspondingly increased 37% with glenoid lateralization, and up to 117% with an onlay humeral construct.

Discussion: Increased lateralization of the glenoid component resulted in increased levels of deltoid and acromial stress. For a given amount of glenoid lateralization, utilization of an inlay stem decreased acromial and deltoid stresses compared to onlay constructs. These data allow surgeons to better understand the interactions of glenoid and humeral lateralization and distalization in the setting of contemporary RSA systems. Level of Evidence: Basic Science Study: Computer Modeling.

Keywords

Reverse shoulder arthroplasty, finite element modeling, acromion fracture risk, deltoid

Date received: 28 March 2024; revised: 16 July 2024; accepted: 23 September 2024

Introduction

Reverse shoulder arthroplasty (RSA) is a successful and commonly performed procedure used to address advanced rotator cuff arthropathy, severe glenohumeral arthritis, proximal humerus fractures, and other expanding indications.^{1–3} RSA can reduce pain and improve function for many patients with durable long-term outcomes,^{4–6} but there are unique complications that can lead to poorer outcomes following this procedure.^{7–9} Complications such as dislocation, acromial stress fractures, nerve injury, and persistent soft tissue pain are more common following RSA when compared to anatomic total shoulder arthroplasty or hemiarthroplasty.¹⁰ These

complications are likely secondary to the unique design features of RSA, as well as the patient population for which the procedure is commonly indicated.¹¹

Surgeons are now presented with a multitude of options for component combinations when considering RSA constructs for their patients. Traditional (Grammont) RSA designs

¹Department of Orthopedics and Rehabilitation, The University of Iowa, Iowa City, USA

Corresponding author:

Brendan M Patterson, 200 Hawkins Drive, Iowa City, IA 52242.
Email: brendan-patterson@uiowa.edu



medialized and distalized the center of rotation of the reconstructed glenohumeral joint.¹² More contemporary RSA design constructs have focused on increased glenoid lateralization to improve impingement-free range of motion.^{13–16} Glenoid component lateralization has been shown in multiple studies to improve impingement-free range of motion, most notably with internal rotation, external rotation, and adduction following RSA.^{13,17,18} In addition to improvements in impingement-free range of motion, glenoid component lateralization and a more varus humeral neck shaft angle protect against scapular notching.^{14,19,20}

Humeral component designs now feature both inlay and onlay constructs that effect both distalization and lateralization of the humerus.^{20–22} Distalization of the humerus has been shown to improve the efficiency of the deltoid and allow the deltoid to act as the primary force generator for forward elevation in patients following RSA.²³ Humeral lateralization is also thought to aid in deltoid wrap and contribute to joint stability following RSA.²⁴ While glenoid component lateralization or humeral component distalization and lateralization may allow surgeons to influence functional/mechanical outcomes following RSA, associated altered stresses in the surrounding soft tissue and bony structures could potentially contribute to the post-operative complications. The effects of combined glenoid lateralization and

humeral lateralization and distalization on acromial and deltoid stresses and joint stability, are not completely understood. Therefore, the main purpose of this study was to evaluate changes in deltoid and acromial stresses with variations in glenoid lateralization, and with inlay versus onlay humeral component designs with a 135° neck-shaft angle in RSA. Furthermore, this study also aimed to investigate the changes in torque requirements for rotating the reconstructed glenohumeral joint with variations in glenoid lateralization, and inlay versus onlay humeral component designs in RSA. Finite element (FE) analyses were undertaken to provide these important mechanical indicators of outcome.

Materials and Methods

Details of our FE modeling approach have been previously described.^{17,25} The fundamental FE model setup (material properties, contact algorithm, constraints, explicit solver) was based on a prior validated model of scapula-liner contact.²⁶ Briefly, model anatomic geometries were acquired from the female shoulder CT scans of the Visible Human Project (Figure 1). The modeling relied upon the middle deltoid and subscapularis tendon to provide tension and soft-tissue restraint around the joint. The setup replicated the clinical case of advanced rotator cuff arthropathy, and only the

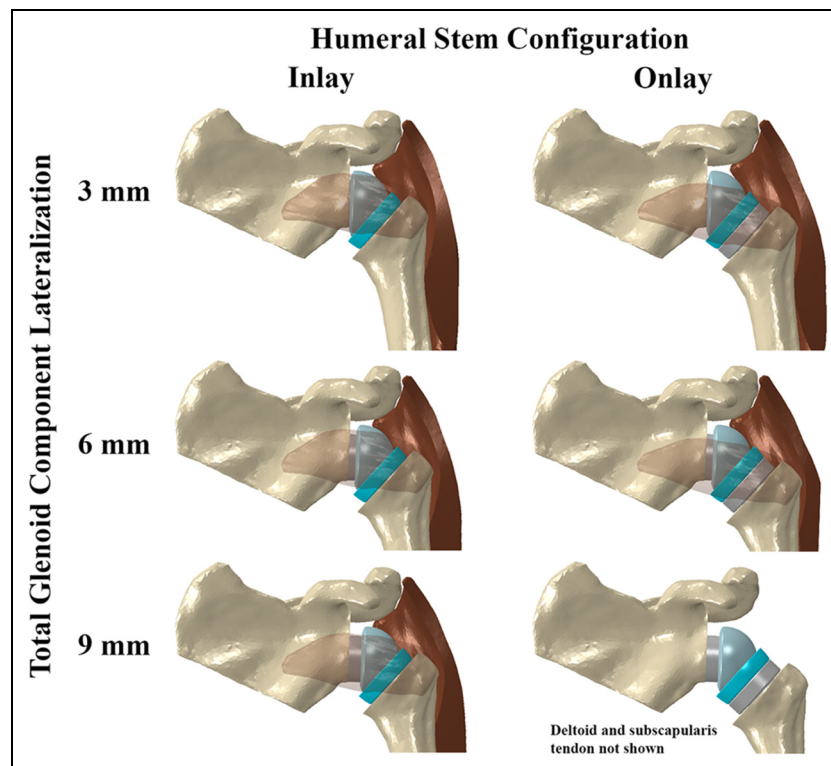


Figure 1. RSA models incorporating the inlay and onlay constructs shown with baseplate and lateralized glenosphere combinations providing up to 9 mm of total glenoid lateralization. The subscapularis tendon is shown transparent for clarity. Note the additional stretch in the subscapularis tendon with glenoid lateralization and onlay construct. The inferior scapula was not included in the model for computational efficiency.

middle deltoid and subscapularis were included as they provided the primary restraint during the simulated motion. The existing RSA FE model was modified to incorporate a generalized representation of the Stryker Tornier Perform[®] RSA system (Stryker, Kalamazoo, MI) with both inlay and onlay configurations (Figure 1). The RSA components included a 25 mm baseplate (standard (0 mm), 3 mm, 6 mm lateralization), 36 mm glenosphere (standard, lateralized (3 mm)), 36 mm 0 mm thickness symmetric liner (135° angle of inclination), and a 9 mm spacer to model the onlay configuration. We used a single RSA system to remove the influence of implant design across parametric comparisons. Glenoid components were placed in ~5° of inferior tilt and neutral version, while the humeral components were placed in ~20° of retroversion. Implant placement was verified by a fellowship-trained shoulder surgeon.

All geometries were meshed using linear tetrahedral elements (3-matic, Materialise, Leuven, Belgium). Tissue- and implant-specific material properties were assigned as previously described.^{17,25} To evaluate acromial stresses, external and internal scapula elements were assigned representative scapula-specific cortical ($E = 9$ GPa) and trabecular ($E = 1$ GPa) bone material properties, respectively.²⁷ Ideally, bone is assigned heterogeneous properties based on CT attenuation. However, we were currently limited to homogeneous material assignment due to the low acquisition/reconstruction quality of the CT scans. Deltoid elements were assigned $E = 10$ MPa.²⁸ Subscapularis tendon elements were assigned $E = 100.5$ MPa.²⁵ The subscapularis tendon and deltoid were rigidly attached to the humerus at their anatomic insertion sites. Simulations were performed in two stages. In the first stage, the subscapularis tendon and deltoid were tensioned and wrapped around the reconstructed glenohumeral joint. This tension was purely a result of the passive stretching of soft tissues relative to the tissue length at the time of CT scanning, which was assumed to be the resting length. Thus, the amount of tensioning directly depended upon the implant lateralization/distalization combinations (and assumed material behavior), since the proximal locations of the soft tissues (corresponding to CT scan locations) were the same across all configurations (Figure 1). In the second stage, we simulated 50° of humeral external rotation from neutral orientation based on range of motion clinically observed in patients after RSA. Due to the variability in muscle integrity observed in patients indicated for RSA, instead of prescribing torques/moments, external rotation was kinematically simulated and subsequent joint torques were measured.²⁵ During rotation simulation, the proximal deltoid was tied to the lateral acromion to allow stress transfer across the soft tissue-bone interface, while the proximal subscapularis tendon was free to move along its length. Uniform deltoid and subscapularis muscle forces,²⁹ were also prescribed at the lateral acromion and proximal subscapularis along their respective lines of action. This was to account for the contribution of active muscle forces to the acromial stresses

during rotation, in addition to the stresses developed from passive tension. The scapula (except for the acromion and inferior glenoid neck/scapular notching regions), baseplate, and glenosphere were fixed during both simulation stages. Contact interactions were defined during both simulation stages between surfaces expected to be involved in contact *in vivo*.^{17,25}

All simulations were performed using a dynamic, explicit FE solver (Abaqus 2018, Dassault Systemes Simulia, Johnston, RI). This dynamic analysis approach allowed for simulation of liner impingement, if any, and rotation beyond impingement and subsequent post-impingement subluxation/instability. Based on baseplate-glenosphere combinations, we evaluated variations in total glenoid lateralization from 3 to 9 mm using the lateralized glenosphere (3 configurations), and variations in total glenoid lateralization from 3 to 6 mm using the standard glenosphere (2 configurations). Note that 9 mm of lateralization achieved through the combination of the lateralized sphere with the 6 mm lateralized baseplate is beyond the recommended combinations in the manufacturer's device labeling. Each lateralized glenoid configuration was evaluated with either the inlay or onlay (with spacer) humeral construct, resulting in 10 total parametric variations. Average deltoid and acromial-scapular spine stresses were determined after virtual implantation of the glenoid and humeral components (tensioned state before rotation), as well as during external rotation. Due to the higher stress magnitudes in the cortical region and likelihood of fracture initiation within this region based on loading mechanics, we focused our results only on the acromial-scapular spine cortical region. Results from the trabecular region showed the same trends. We also determined percent change in stress at implantation across configurations compared to a reference configuration. The standard baseplate and lateralized glenosphere combination (3 mm total glenoid lateralization) with inlay construct was selected as the reference configuration because most surgeons use some glenoid lateralization with this stem given the 135° angle of inclination. A medialized construct would be very uncommon and not often recommended with this stem. The torques required to externally rotate the humerus with simulated subscapularis repair immediately prior to impingement and any subsequent post-impingement subluxation were determined for each implant configuration. Subluxation was calculated as the gap distance between the glenosphere and liner centers of rotation.^{17,25}

Results

Deltoid Stress:

After virtual implantation of RSA components (ie, before rotation), increasing glenoid lateralization alone resulted in progressive stretching of the deltoid as expected (Figure 2). In an inlay configuration, compared to the reference construct

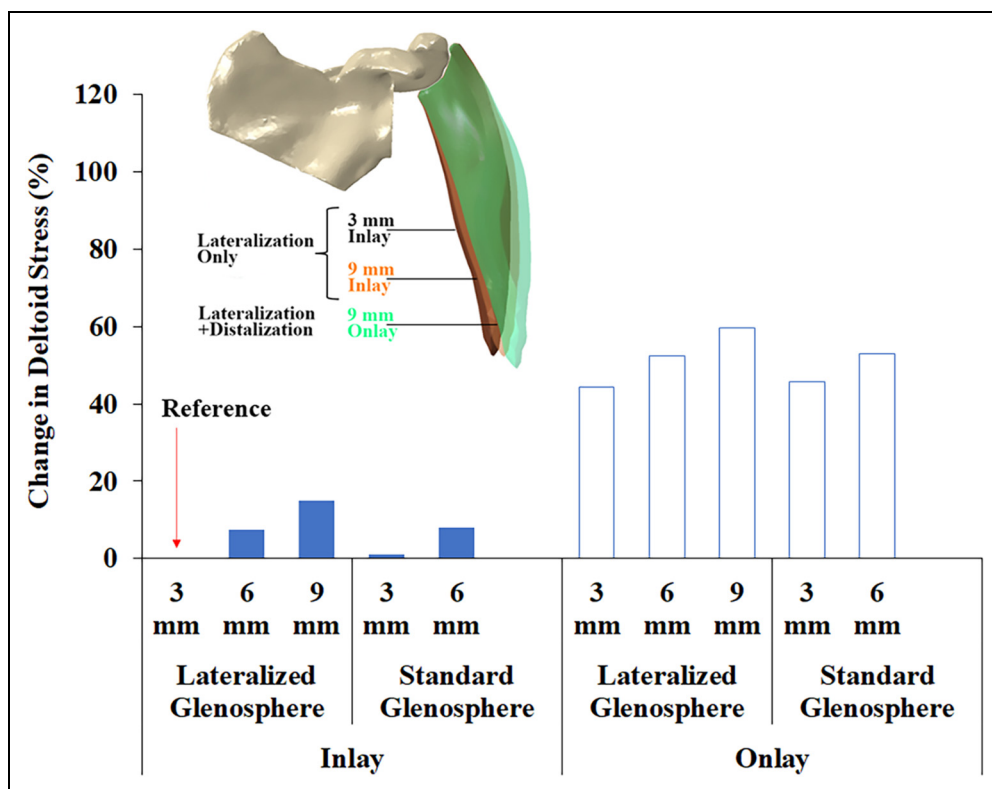


Figure 2. Change in deltoid stresses at implantation (before rotation) with total glenoid lateralization from 3 mm to 9 mm, and inlay versus onlay humeral stem designs. Inset shows the more severe deltoid stretching that occurred with the onlay construct.

of 3 mm total glenoid lateralization, deltoid stress increased 15% for the most lateralized construct of 9 mm of total glenoid lateralization. Deltoid stress increased 7.4% when glenoid lateralization was increased from 3 mm to 6 mm and an additional 7.5% when glenoid lateralization increased from 6 mm to 9 mm. On the other hand, deltoid stress increased substantially with distalization and lateralization of the humerus using the onlay construct due to stretching along the muscle axis (Figure 2). For example, deltoid stress increased 39% when changing constructs from the inlay to the onlay configuration at maximal glenoid lateralization of 9 mm. Similar patterns of deltoid stress were also observed during external rotation of the reconstructed glenohumeral joint (Figure 3).

Acromial Stress:

In association with deltoid stretching, acromial stress was found to correspondingly increase with glenoid lateralization, and humeral distalization and lateralization after virtual implantation (Figure 4). In an inlay configuration, acromial stress increased up to 37% with maximal glenoid lateralization of 9 mm compared to the reference glenoid lateralization of 3 mm at implantation. Secondary to increased humeral distalization and lateralization, acromial stress increased even more so with the use of an onlay humeral construct.

Acromial stress increased up to 117% with use of maximal glenoid lateralization of 9 mm and an onlay humeral stem construct. Glenoid lateralization increased acromial stress also during external rotation, and the addition of an onlay humeral component further increased acromial stress during simulated external rotation (Figure 5). At the same level of lateralization, stresses for constructs incorporating the standard glenosphere were similar to those for constructs incorporating the lateralized glenosphere. The anatomic location of high acromial stress was found to be focused along the middle portion of the scapular spine as well as the distal most aspect of the supraspinatus fossa (Figure 6). Larger regions of the acromion and scapula spine experienced higher stresses with use of an onlay stem.

Torque Prior to Impingement:

There was a 24% increase in torque as total glenoid lateralization increased from 3 mm to 9 mm (lateralized glenosphere combinations) with the inlay construct (Figure 7). The torque required to externally rotate the humerus increased at each level of glenoid lateralization with the addition of an onlay humeral stem design, though the increases were relatively low (for example, 8.4%, 2.9%, and 4.4% with total glenoid lateralization of 3 mm, 6 mm, and 9 mm, respectively, using the lateralized glenosphere construct).

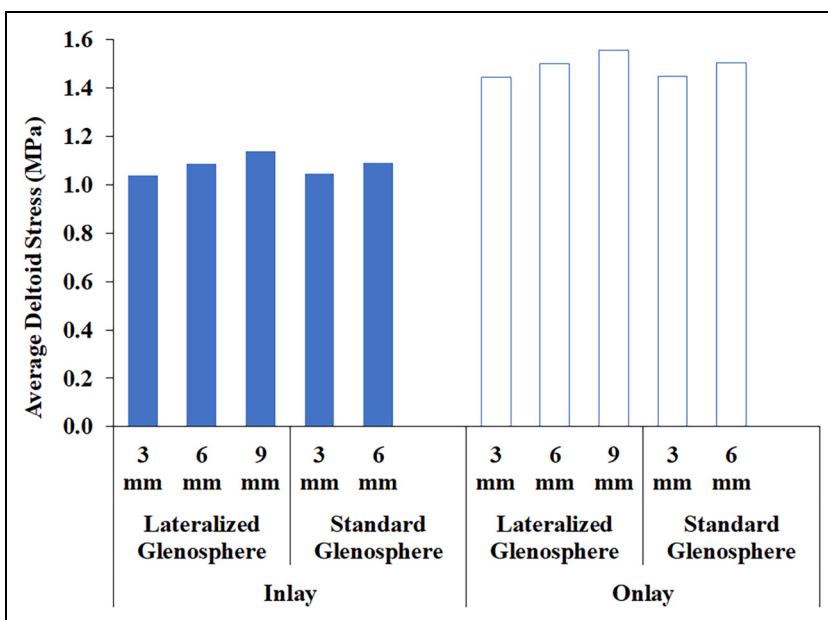


Figure 3. Variations in deltoid stresses during external rotation with total glenoid lateralization from 3 mm to 9 mm and inlay versus only humeral stem designs.

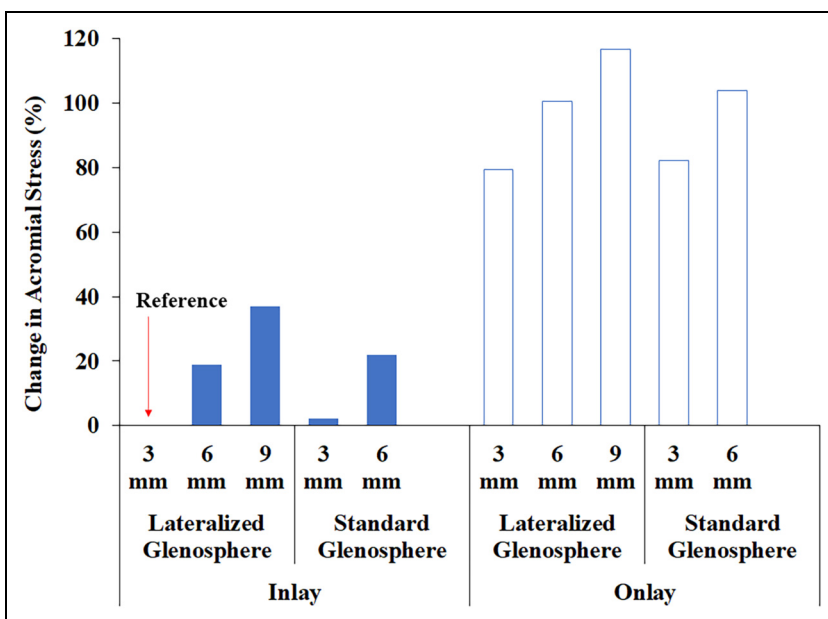


Figure 4. Change in acromial stresses at implantation (before rotation) with total glenoid lateralization from 3 mm to 9 mm and inlay versus only humeral stem designs.

Post-Impingement Subluxation:

The use of an onlay stem decreased the impingement-related subluxation gap distances at terminal external rotation for all levels of glenoid lateralization modeled except for 9 mm of glenoid lateralization (Figure 8), where impingement occurred at 50° of external rotation. The reduction in

subluxation was more pronounced for the onlay construct with 3 mm of glenoid lateralization as subluxation increased proportionately with prolonged rotation after impingement, which occurred earlier in the range of external rotation (35° and 37.5° for the lateralized and standard glenosphere combinations, respectively).

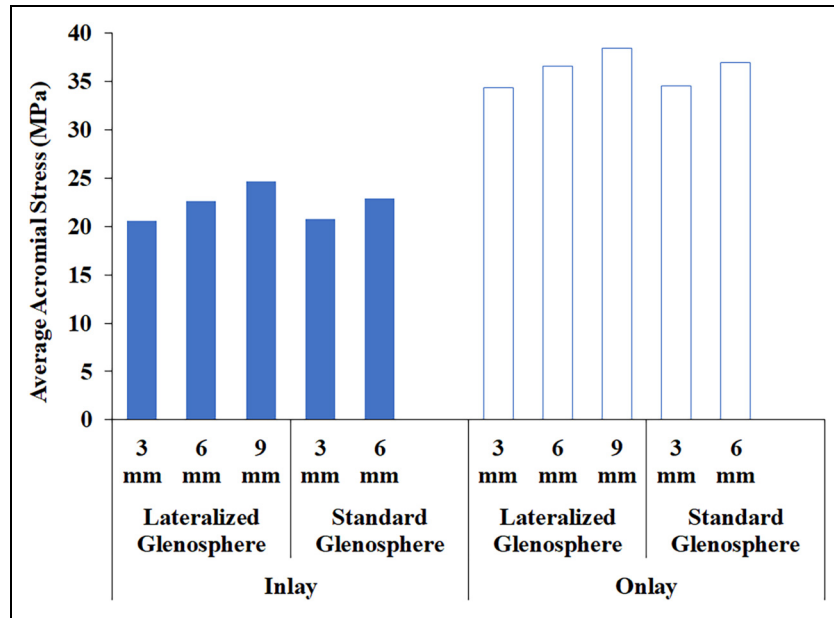


Figure 5. Variations in acromial stresses during external rotation with total glenoid lateralization from 3 mm to 9 mm and inlay versus onlay humeral stem designs.

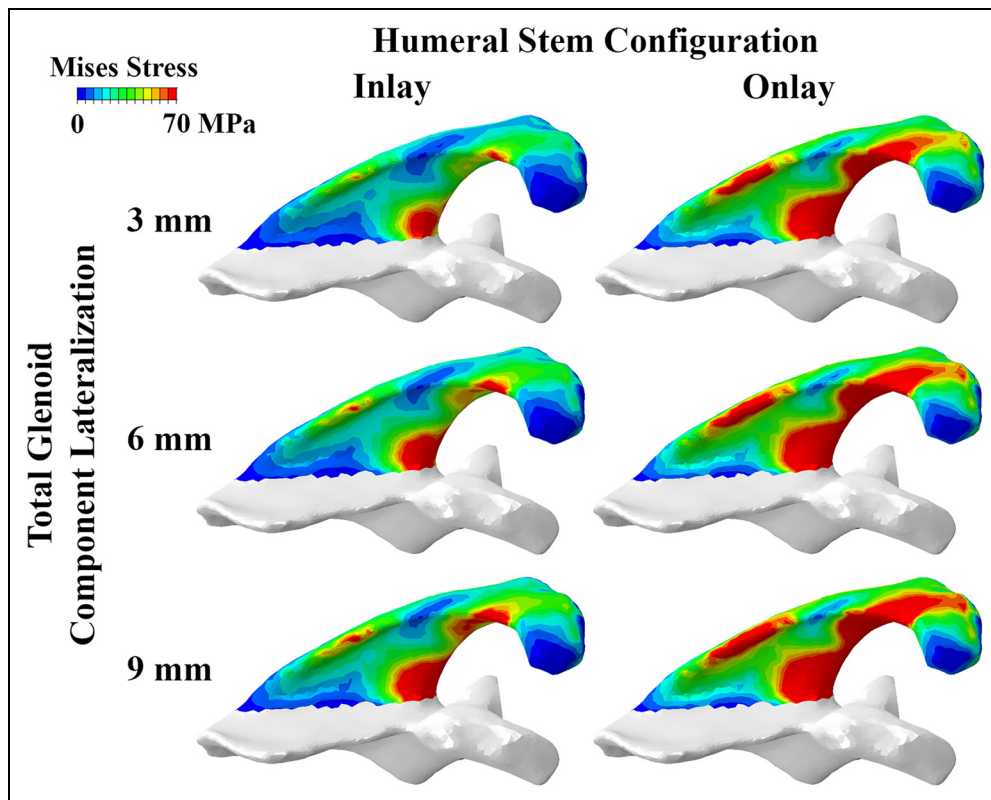


Figure 6. Scapular spine and acromial von Mises stress distributions at implantation shown for constructs incorporating inlay and onlay stems and progressive amounts of glenoid component lateralization (total 3 mm to 9 mm with the lateralized glenosphere). Stress distributions for constructs incorporating the standard glenosphere (not shown) were similar at the corresponding lateralization level.

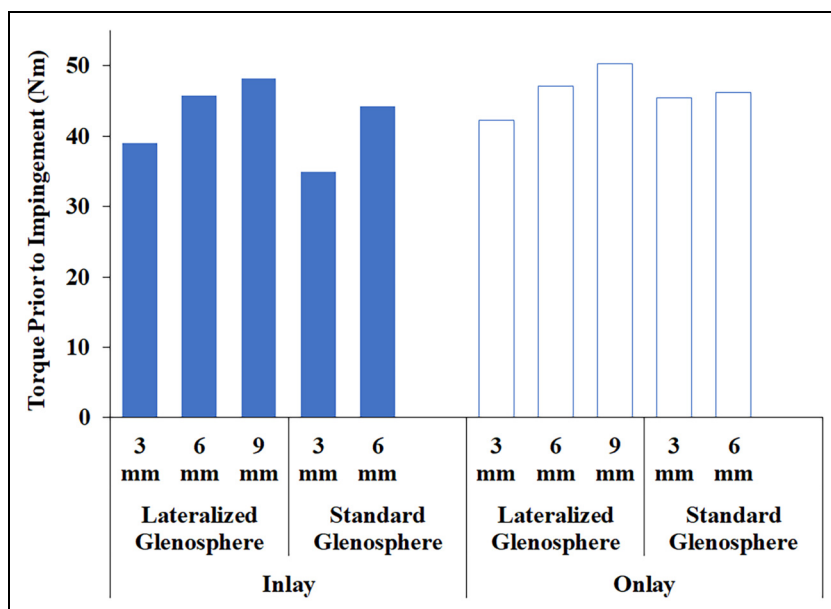


Figure 7. Torque requirements for the simulated external rotation of the humerus with variations in glenoid lateralization from 3 mm to 9 mm and with inlay versus onlay humeral stem designs.

Discussion

Increased lateralization of the glenoid component resulted in increased levels of deltoid and acromial stress in RSA as expected. For a given amount of glenoid component lateralization, the utilization of an inlay stem substantially decreased acromial and deltoid stress as compared to onlay stem constructs. Increased soft tissue tension from glenoid lateralization and humeral distalization was observed to increase torque requirements for external rotation. However, it was also observed to decrease subluxation associated with impingement during maximal external rotation.

The results of this study are consistent with previously published cadaveric research that has described increased deltoid stresses with glenoid lateralization.^{24,30} Ott et al investigated glensphere size and glenoid component lateralization in a cadaveric RSA model and found that increased glenoid component lateralization increased deltoid stresses regardless of glensphere size.³⁰ Giles et al investigated both humeral and glenoid component lateralization in a biomechanical cadaveric model using an RSA configuration with a humeral neck shaft angle of 155° and varying amounts of glenoid and humeral lateralization.²⁴ Consistent with our results, increased levels of glenoid lateralization resulted in increased deltoid forces in their cadaveric model. The results of our FE model were also consistent with their study in that we too found increased joint kinetics with modification on the humeral side from an inlay to onlay design. Our results add to the literature in that in our model, a 135° neck shaft angle was utilized. Many contemporary RSA design features now allow for a more varus neck shaft angle as compared to the traditional Grammont style RSA. A more varus neck

shaft angle has been shown to improve rotational impingement free ROM, thus we felt it important to test a 135° neck shaft angle stem in this model.¹³

In addition to investigating the effects of deltoid stresses, we also wanted to determine relative changes in acromial stress and the location of those stresses on the acromion and scapular spine. As the rate of RSA continues to increase, surgeons are now forced to understand and manage the complications associated with RSA with increased frequency.^{31,32} Acromial stress fractures are a rare yet problematic complication that is relatively unique to RSA.³³ The rate of acromial stress fracture following RSA is estimated between 1–7%.^{34–36} Acromial stress reactions and fractures can have significant negative effects on overall functional outcome following RSA.³³ Risk factors for developing acromial fractures following RSA include female sex, rheumatoid arthritis, older age, osteoporosis, and rotator cuff tear arthropathy.³⁷ In addition to patient factors that are known to increase the risk of acromial stress fractures following RSA, certain implant characteristics may also contribute to the development of this potential complication. Routman et al found an association between increased number of baseplate screws and acromial stress fractures following RSA.³³ King et al, in a meta-analysis of acromial stress fractures after RSA, found that a medialized glenoid construct combined with a lateralized humeral construct resulted in the lowest rate of acromial stress fracture.³⁵ Wong et al demonstrated increased acromial stresses in a computational model with increased levels of glenoid component lateralization.³⁸ Our results are consistent with those reported by Wong et al, in that increased glenoid component lateralization also resulted in increased acromial stress in our model.

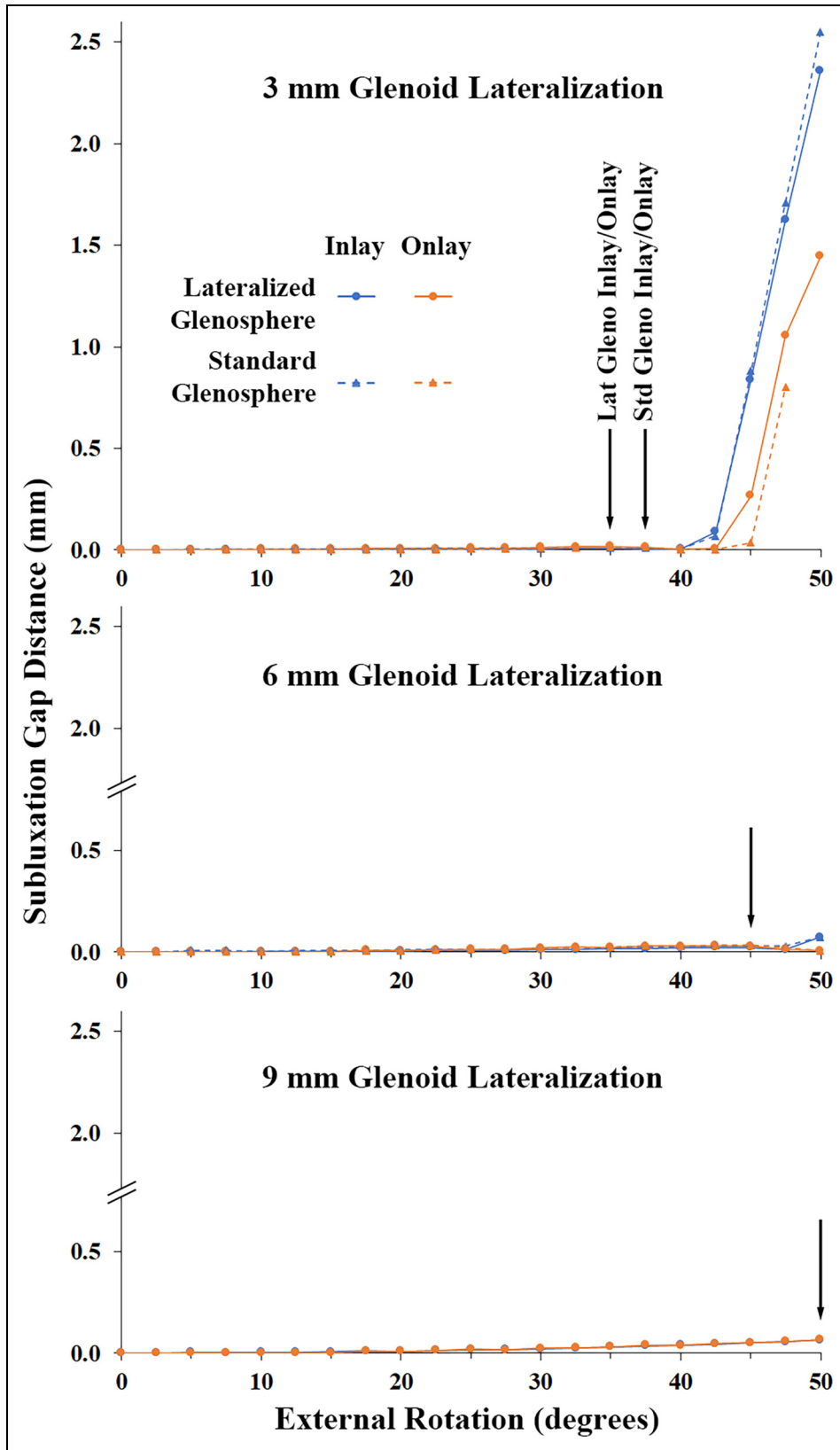


Figure 8. Variations in subluxation gap distances during external rotation for all implant configurations. Arrows indicate the external rotation angle at which liner impingement occurred.

Furthermore, by investigating humeral lengthening, our model highlights the important interplay between glenoid lateralization and humeral distalization. For any given amount of glenoid lateralization, additional humeral distalization, resulted in greater amounts of acromial stresses. With maximal glenoid lateralization and the use of an onlay humeral stem configuration, maximal acromial stress was encountered at the midportion of the scapular spine. Levy et al classified acromial fractures following RSA based on the location along the acromion and scapular spine.³⁹ Levy noted that 50% of fractures in their series were type 2 fractures. The location of stress encountered along the scapular spine has important clinical relevance based on our prior understanding of the pathoanatomy of acromial stress fractures. Given increased amounts of deltoid and acromial stress with variations in glenoid lateralization and humeral distalization, it would follow that different patients would likely benefit from more or less glenoid lateralization and/or humeral distalization depending on their risk factors for acromial stress fracture and/or dislocation.

The FE modeling approach used also allowed for assessments of torque required to externally rotate the reconstructed glenohumeral joint prior to impingement, and post-impingement subluxation gap distances. Greater tensioning of the soft-tissue structures that accompanies the additional distalization and lateralization with the onlay construct helped to provide stability in the reconstructed joint against subluxation during rotation after impingement. However, improvement in post-impingement stability comes with the trade-off of increased torque demand due to increased joint stiffness, which may hinder the achievable post-operative range of motion. Progressive glenoid lateralization has been previously shown to increase the torque required to externally rotate the shoulder after RSA, particularly with repair of a stiffer subscapularis.²⁵ As expected, the addition of an onlay stem had a relatively lesser effect on torque compared to deltoid and acromial stresses due to the incremental (mm) change in the distance from the center of rotation as opposed to the substantial deformation of the soft tissues.

Several limitations of our study deserve mention. Only passive tension was considered, which in our current model setup, is a function of initial CT geometry length, assigned soft-tissue material property, and implant combination. While the model setup of passive tension would provide an appropriate assessment of mechanical changes and associated risks for the selected implant configuration immediately after surgery, it is important that the model inputs capture realistic patient characteristics for accurate interpretation. In the clinical setting, standardized CT scans are typically acquired for pre-operative surgical planning. Patient-specific muscle integrity could potentially be estimated from concurrent MRI scans and empirical stiffness relationships.⁴⁰ Though we were restricted to a homogeneous material assignment due to insufficient CT quality, CT-derived heterogeneous bone material can be implemented on a patient basis, which in this study was approximated using representative

scapula region-specific values.²⁷ While our FE model was based on a prior validated model of scapular notching,²⁶ our computational evaluation of acromial stress based on initial soft-tissue geometry and material property assumptions needs further validation that is beyond the scope of the current study. Though stress magnitudes could vary with tissue heterogeneity in RSA patients, the interpretation of our results is expected to be consistent due to the parametric assessment of implant configurations. Despite the underlying assumptions related to soft-tissue geometry and material property, our stress magnitudes were reasonable and corresponded well with published values,³⁸ and the location of high stresses on the scapular spine corroborated well with the clinically observed common location of post-operative acromial stress fractures (Levy Type II).³⁹ Upon validation of our computed stresses, the magnitude and location of high stresses could be used to estimate prospective mechanical fracture risk for a given RSA construct at the time of implantation. For example, based on the empirically known yield strain of bone (0.62% in tension),⁴¹ the scapular regions experiencing high stresses (>70 MPa; Figure 6) would exceed the yield strength limit (56 MPa, for the assumed scapula-specific cortical material), potentially placing them at a higher risk of fracture. Also, post-RSA mechanics may change over time with muscle remodeling and additional stresses may occur from active muscle contraction, which was not simulated. Implementing active muscle forces as a function of motion, in addition to passive tension, is a future goal. The evaluation of a single motion was another limitation, and we did not presently model the posterior cuff. Our model simulated the scenario of cuff tear arthropathy with a deficient cuff, and stress magnitudes and distribution may vary with an intact cuff and other motions, which is a topic for further investigation.

Despite these limitations, our model allows for dynamic, and post-impingement evaluation of stresses during motion, which may provide a more comprehensive understanding of post-operative RSA mechanics. Higher bone stresses were observed during rotation after impingement due to soft-tissue stretching from buttressing of post-impingement humerus subluxation, which could potentially be better captured with a dynamic analysis including soft-tissue structures, compared to studies that simulate direct application of quasi-static forces excluding soft-tissues.³⁸ These data may allow surgeons to better understand the interactions of glenoid lateralization and humeral distalization in the setting of contemporary RSA systems. An appreciation of these factors will assist surgeons' component selection when contemplating glenoid component lateralization and/or humeral distalization in RSA. Future investigation will further define these relationships and add to the understanding of how component positioning effects the mechanics of RSA. Hopefully such efforts will lead to optimization of implant selection and improvement in design which will improve patient outcomes.

Conclusion

Increased lateralization of the glenoid component resulted in increased levels of deltoid and acromial stress in RSA. For a given amount of glenoid component lateralization, the utilization of an inlay stem decreased acromial and deltoid stress as compared to onlay stem constructs. This data allows surgeons to better understand the interactions of glenoid lateralization and humeral distalization and lateralization in the setting of contemporary RSA systems. An appreciation of these factors can assist surgeons in component selection when contemplating glenoid component lateralization and/or humeral distalization in RSA.

Acknowledgements

Funding for this research and implant geometries were provided by Stryker Orthopedics.

Author Contributors

Brendan M. Patterson, MD: conceptualization, investigation, writing (original draft), project administration.

Joshua E. Johnson, PhD: methodology, software, investigation, writing (original draft), visualization.

Maria F. Bozoghlian, MD: investigation, writing (review and editing), project administration.

Donald D. Anderson, PhD: conceptualization, methodology, validation, writing (review and editing), supervision.

Declaration of Conflicting Interests


The authors declared no potential conflicts of interest with respect to the research, authorship, and/or publication of this article.

Funding

The authors disclosed receipt of the following financial support for the research, authorship, and/or publication of this article: This study received ethical approval from the University of Iowa IRB (approval # 202104711) on 05/28/2021.

ORCID iDs

Maria Bozoghlian  <https://orcid.org/0000-0002-9729-0926>

Donald D Anderson  <https://orcid.org/0000-0002-1640-6107>

References

1. Kozak T, Bauer S, Walch G, et al. An update on reverse total shoulder arthroplasty: current indications, new designs, same old problems. *EFORT Open Rev.* 2021;6(3):189–201. DOI:10.1302/2058-5241.6.200085
2. Familiari F, Rojas J, Nedim Doral M, et al. Reverse total shoulder arthroplasty. *EFORT Open Rev.* 2018;3(2):58–69. DOI:10.1302/2058-5241.3.170044
3. Chalmers PN, Keener JD. Expanding roles for reverse shoulder arthroplasty. *Curr Rev Musculoskelet Med.* 2016;9(1):40–48. DOI:10.1007/s12178-016-9316-0
4. Chelli M, Boileau P, Domos P, et al. Survivorship of reverse shoulder arthroplasty according to indication, age and gender. *J Clin Med.* 2022;11(10). DOI:10.3390/jcm11102677
5. Bulhoff M, Zeifang F, Welters C, et al. Medium- to long-term outcomes after reverse total shoulder arthroplasty with a standard long stem. *J Clin Med.* 2022;11(9). DOI: 10.3390/jcm11092274
6. Kennedy J, Klifto CS, Ledbetter L, et al. Reverse total shoulder arthroplasty clinical and patient-reported outcomes and complications stratified by preoperative diagnosis: a systematic review. *J Shoulder Elbow Surg.* 2021;30(4):929–941. DOI:10.1016/j.jse.2020.09.028
7. Galvin JW, Kim R, Ment A, et al. Outcomes and complications of primary reverse shoulder arthroplasty with minimum of 2 years' follow-up: a systematic review and meta-analysis. *J Shoulder Elbow Surg.* 2022;31(11):e534–e544. DOI:10.1016/j.jse.2022.06.005
8. Shah SS, Gaal BT, Roche AM, et al. The modern reverse shoulder arthroplasty and an updated systematic review for each complication: part I. *JSES Int.* 2020;4(4):929–943. DOI:10.1016/j.jseint.2020.07.017
9. Shah SS, Roche AM, Sullivan SW, et al. The modern reverse shoulder arthroplasty and an updated systematic review for each complication: part II. *JSES Int.* 2021;5(1):121–137. DOI:10.1016/j.jseint.2020.07.018
10. Scarlat MM. Complications with reverse total shoulder arthroplasty and recent evolutions. *Int Orthop.* 2013;37(5):843–851. DOI:10.1007/s00264-013-1832-6
11. Patterson BM, Reed ER, Hill E, et al. Increasing awareness of complications of nerve injury following shoulder surgery: preventing delays in referral and treatment. *HAND.* 2024;19(3):352–360. DOI:10.1177/15589447221142886
12. Boileau P, Watkinson DJ, Hatzidakis AM, et al. Grammont reverse prosthesis: design, rationale, and biomechanics. *J Shoulder Elbow Surg.* 2005;14(1 Suppl S):147S–161S. DOI:10.1016/j.jse.2004.10.006
13. Keener JD, Patterson BM, Orvets N, et al. Optimizing reverse shoulder arthroplasty component position in the setting of advanced arthritis with posterior glenoid erosion: a computer-enhanced range of motion analysis. *J Shoulder Elbow Surg.* 2018;27(2):339–349. DOI:10.1016/j.jse.2017.09.011
14. Parry S, Stachler S, Mahylis J. Lateralization in reverse shoulder arthroplasty: a review. *J Orthop.* 2020;22:64–67. DOI:10.1016/j.jor.2020.03.027
15. Mulieri P, Dunning P, Klein S, et al. Reverse shoulder arthroplasty for the treatment of irreparable rotator cuff tear without glenohumeral arthritis. *J Bone Joint Surg Am.* 2010;92(15):2544–2556. DOI:10.2106/JBJS.I.00912
16. Frankle M, Levy JC, Pupello D, et al. The reverse shoulder prosthesis for glenohumeral arthritis associated with severe rotator cuff deficiency. a minimum two-year follow-up study of sixty patients surgical technique. *J Bone Joint Surg Am.* 2006;88(Suppl 1 Pt 2):178–190. DOI:10.2106/JBJS.F.00123
17. Johnson JE, Caceres AP, Anderson DD, et al. Postimpingement instability following reverse shoulder arthroplasty: a parametric finite element analysis. *Semin Arthroplasty.* 2021;31(1):36–44. DOI:10.1053/j.sart.2020.10.005
18. Kim SJ, Jang SW, Jung KH, et al. Analysis of impingement-free range of motion of the glenohumeral joint after reverse total shoulder arthroplasty using three different implant models. *J Orthop Sci.* 2019;24(1):87–94. DOI:10.1016/j.jos.2018.08.016
19. Cogan CJ, Ho JC, Entezari V, et al. The influence of reverse total shoulder arthroplasty implant design on biomechanics.

- Curr Rev Musculoskelet Med.* 2023;16. DOI:10.1007/s12178-023-09820-8
20. Wright MA, Murthi AM. Offset in reverse shoulder arthroplasty: where, when, and how much. *J Am Acad Orthop Surg.* 2021;29(3):89–99. DOI:10.5435/JAAOS-D-20-00671
 21. Ladermann A, Denard PJ, Collin P, et al. Effect of humeral stem and glenosphere designs on range of motion and muscle length in reverse shoulder arthroplasty. *Int Orthop.* 2020;44(3):519–530. DOI:10.1007/s00264-019-04463-2
 22. Larose G, Fisher ND, Gambhir N, et al. Inlay versus onlay humeral design for reverse shoulder arthroplasty: a systematic review and meta-analysis. *J Shoulder Elbow Surg.* 2022;31(11):2410–2420. DOI:10.1016/j.jse.2022.05.002
 23. Walker DR, Kinney AL, Wright TW, et al. How sensitive is the deltoid moment arm to humeral offset changes with reverse total shoulder arthroplasty? *J Shoulder Elbow Surg.* 2016;25(6):998–1004. DOI:10.1016/j.jse.2015.10.028
 24. Giles JW, Langohr GD, Johnson JA, et al. Implant design variations in reverse total shoulder arthroplasty influence the required deltoid force and resultant joint load. *Clin Orthop Relat Res.* 2015;473(11):3615–3626. DOI:10.1007/s11999-015-4526-0
 25. Linderman SE, Johnson JE, Anderson DD, et al. Influence of subscapularis stiffness with glenosphere lateralization on physiological external rotation limits after reverse shoulder arthroplasty. *J Shoulder Elbow Surg.* 2021;30(11):2629–2637. DOI:10.1016/j.jse.2021.04.039
 26. Permeswaran VN, Goetz JE, Rudert MJ, et al. Cadaveric validation of a finite element modeling approach for studying scapular notching in reverse shoulder arthroplasty. *J Biomech.* 2016;49(13):3069–3073. DOI:10.1016/j.jbiomech.2016.07.007
 27. Chae SW, Lee H, Kim SM, et al. Primary stability of inferior tilt fixation of the glenoid component in reverse total shoulder arthroplasty: a finite element study. *J Orthop Res.* 2016;34(6):1061–1068. DOI:10.1002/jor.23115
 28. Kot BC, Zhang ZJ, Lee AW, et al. Elastic modulus of muscle and tendon with shear wave ultrasound elastography: variations with different technical settings. *PLoS One.* 2012;7(8):e44348. DOI:10.1371/journal.pone.0044348
 29. Hughes RE, An KN. Force analysis of rotator cuff muscles. *Clin Orthop Relat Res.* 1996;330:75–83. DOI:10.1097/00003086-199609000-00010
 30. Ott N, Alikah A, Hackl M, et al. The effect of glenoid lateralization and glenosphere size in reverse shoulder arthroplasty on deltoid load: a biomechanical cadaveric study. *J Orthop.* 2021; 25:107–111. DOI:10.1016/j.jor.2021.04.007
 31. Cheung E, Willis M, Walker M, et al. Complications in reverse total shoulder arthroplasty. *J Am Acad Orthop Surg.* 2011; 19(7):439–449.
 32. O'Reilly OC, Day MA, Skalitzky MK, et al. Utilization of reverse shoulder arthroplasty for the treatment of glenohumeral arthritis among American Board of Orthopaedic Surgery (ABOS) Part II candidates, 2008–2019. *Semin Arthroplasty.* 2022;32(1):55–62. DOI:10.1053/j.sart.2021.06.005
 33. Routman HD, Simovitch RW, Wright TW, et al. Acromial and scapular fractures after reverse total shoulder arthroplasty with a medialized glenoid and lateralized humeral implant: an analysis of outcomes and risk factors. *J Bone Joint Surg Am.* 2020;102(19):1724–1733. DOI:10.2106/JBJS.19.00724
 34. Zumstein MA, Pinedo M, Old J, et al. Problems, complications, reoperations, and revisions in reverse total shoulder arthroplasty: a systematic review. *J Shoulder Elbow Surg.* 2011;20(1):146–157. DOI:10.1016/j.jse.2010.08.001
 35. King JJ, Dalton SS, Gulotta LV, et al. How common are acromial and scapular spine fractures after reverse shoulder arthroplasty?: a systematic review. *Bone Joint J.* 2019;101-B(6):627–634. DOI:10.1302/0301-620X.101B6.BJJ-2018-1187.R1
 36. Hatstrup SJ. The influence of postoperative acromial and scapular spine fractures on the results of reverse shoulder arthroplasty. *Orthopedics.* 2010;33(5). DOI:10.3928/01477447-20100329-04
 37. Group ACoRR, Mahendraraj KA, Abboud J, et al. Predictors of acromial and scapular stress fracture after reverse shoulder arthroplasty: a study by the ASES Complications of RSA Multicenter Research Group. *J Shoulder Elbow Surg.* 2021;30(10):2296–2305. DOI:10.1016/j.jse.2021.02.008
 38. Wong MT, Langohr GDG, Athwal GS, et al. Implant positioning in reverse shoulder arthroplasty has an impact on acromial stresses. *J Shoulder Elbow Surg.* 2016;25(11):1889–1895. DOI:10.1016/j.jse.2016.04.011
 39. Levy JC, Anderson C, Samson A. Classification of postoperative acromial fractures following reverse shoulder arthroplasty. *J Bone Joint Surg Am.* 2013;95(15):e104. DOI:10.2106/JBJS.K.01516
 40. Giambini H, Hatta T, Rezaei A, et al. Extensibility of the supraspinatus muscle can be predicted by combining shear wave elastography and magnetic resonance imaging-measured quantitative metrics of stiffness and volumetric fat infiltration: a cadaveric study. *Clin Biomech (Bristol, Avon).* 2018;57: 144–149. DOI:10.1016/j.clinbiomech.2018.07.001
 41. Bayraktar HH, Morgan EF, Niebur GL, et al. Comparison of the elastic and yield properties of human femoral trabecular and cortical bone tissue. *J Biomech.* 2004;37(1):27–35. DOI:10.1016/s0021-9290(03)00257-4